SUPPORTING INFORMATION

Biodegradation of Single-Walled Carbon Nanotubes by Eosinophil Peroxidase

Fernando T. Andón[†], Alexandr A. Kapralov[†], Naveena Yanamala, Weihong Feng, Arjang Baygan, Benedict J. Chambers, Kjell Hultenby, Fei Ye, Muhammet S. Toprak, Birgit D. Brandner, Andrea Fornara, Judith Klein-Seetharaman, Gregg P. Kotchey, Alexander Star, Anna A. Shvedova, Bengt Fadeel and Valerian E. Kagan**

Dr. F. T. Andón, Dr. B. Fadeel
Division of Molecular Toxicology, Institute of Environmental Medicine
Karolinska Institutet
Nobel Väg 13, Stockholm, 17177, Sweden
E-mail: bengt.fadeel@ki.se

Dr. A. A. Kapralov, Dr. W. Feng, Dr. V. E. Kagan
Department of Environmental and Occupational Health
University of Pittsburgh
100 Technology Drive, Pittsburgh, PA 15219, USA
E-mail: kagan@pitt.edu

Dr. N. Yanamala
Pathology & Physiology Research Branch
NIOSH, 1095 Willowdale Road, Morgantown, WV 26505, USA

A. Baygan, Dr. B. J. Chambers
Center for Infectious Medicine, Department of Medicine
Karolinska Institutet, Karolinska University Hospital
Stockholm, 17177, Sweden

Dr. K. Hultenby
Clinical Research Center, Department of Laboratory Medicine
Karolinska Institutet, Karolinska University Hospital Huddinge
Stockholm, 14186, Sweden

Dr. F. Ye, Dr. M. S. Toprak
Functional Materials Division, Department of Materials and Nanophysics
Royal Institute of Technology
Stockholm, 16440, Sweden

Dr. B. D. Brandner, Dr. A. Fornara
Institute for Surface Chemistry

Stockholm, 11428, Sweden

Dr. J. Klein-Seetharaman
Department of Structural Biology, University of Pittsburgh School of Medicine
Pittsburgh, PA 15260, USA

G. P. Kotchey, Dr. A. Star
Department of Chemistry
University of Pittsburgh
Pittsburgh, PA 15260, USA

Dr. A. A. Shvedova
Health Effects Laboratory Division
NIOSH, 1095 Willowdale Road, Morgantown, WV 26505, USA
and Department Pharmacology & Physiology
West Virginia University
Morgantown, WV 26505, USA

[†]These authors contributed equally to this work.

*These authors are shared senior and corresponding authors.

Supplementary Material and Methods

1. **Oxidation of single-walled carbon nanotubes (SWCNTs).** Approximately 10 mg of SCWNTs (P2, Carbon Solutions, Inc., Riverside, CA) were sonicated (Branson 1510, frequency 40 kHz) in 20 ml of concentrated H_2SO_4:HNO_3 at a ratio of 3:1 at 70 °C for 40 minutes. After diluting the solution 10-fold with deionized water, the oxidized SWCNTs were first filtered on a 0.22 µm Teflon membrane filter and subsequently washed with copious amounts of water until the pH of the filtrate was ~7.

2. **Incubation of SWCNTs with human EPO.** SWCNTs (15 µg per sample) were incubated with eosinophil peroxidase obtained from human blood (hEPO) (Planta Natural Products, Austria) (concentration 0.5 mg/ml) in 100 mM phosphate buffer (pH 7.4) at 37^{o}C. Aliquots were taken at several time points. H_2O_2 (100 µM) and NaBr (100 µM) were added every 1 h, 5 µl of hEPO was added every 12 h. Total volume of sample was 100 µl.

3. **Assessment of carbon nanotube degradation by hEPO. Transmission Electron Microscopy (TEM).** SWCNTs were suspended in dimethylformamide (DMF) or water *via* sonication for one minute. 5 µl of sample was placed on a lacey carbon grid (Pacific-Grid Tech, San Francisco, CA) and allowed to dry in ambient conditions overnight. Imaging was performed on a FEI Morgagni TEM (80 keV) (Tokyo, Japan). **Infrared spectroscopy (UV-vis-NIR).** hEPO/H_2O_2-mediated oxidative modification of SWCNTs was investigated by ultraviolet visible-near-infrared (UV-vis-NIR) spectrophotometer (Perkin-Elmer, Waltham, MA). Spectra

were recorded using a 45 µl cuvette (Starna Cell Inc, Atascadero, CA). **Raman spectroscopy**. Samples were prepared by drop-casting approximately 30 µl of sample on a microscope slide and allowed to dry. A Renishaw inVia Raman microscope spectrometer (Renishaw, Gloucestershire, UK) with an excitation wavelength of 633 nm was used for all samples, spectrum was obtained over the range of 1000 to 1800 cm^{-1} to visualize D and G band intensity changes throughout the degradation process. Spectra were collected with a 15 second exposure time, at 50% laser power and averaged across 3 scans per sample.

4. **Assessment of peroxidase activity by Amplex Red.** SWCNTs (3 µg/sample) were incubated with 1µl hEPO, 25 µM H_2O_2 and different concentrations of NaBr in 100 mM phosphate buffer (pH 7.4) containing 100 µM DTPA. Final volume was 50 µl. After incubation for 0, 2 or 4 hours, the aliquots of samples were diluted 10 times and residual peroxidase activity of hEPO was measured after addition of Amplex Red (100 µM) and H_2O_2 (100 µM) by fluorescence of resorufin (oxidation product of Amplex Red) (λex-570 nm; λem-585 nm). Fluorescence was measured using a Shimadzu RF5301-PC spectrofluorometer (Shimadzu, Kyoto, Japan).

5. **Computer Modelling. Homology modelling of EPO.** The structural model of EPO was generated using the homology modeling approach with the myeloperoxidase structure as its template. While the sequence for EPO was obtained from swissprot using the id ”P11678”, the sequence corresponding to myeloperoxidase was read directly from its crystal structure (Protein Data Bank code 1MHL). An alignment of the EPO with respect to the myeloperoxidase was generated using ClustalW.[1] With the sequence alignment generated, the three-

dimensional model of EPO was built by homology modeling using the MODELLER software.[2,3] Thus generated structural model of EPO containing both light and heavy chains was used further for performing docking studies with oxidized SWCNTs. **Molecular docking.** Two different types of oxidized SWCNTs were docked to the homology model of EPO using Autodock Vina.[4] The generation details of the structures of the two types of oxidized SWCNTs either at the edge or in the middle was described previously.[5] In brief, SWCNTs with a diameter of 1.1 nm and the chirality parameters m and n of 14 and 0 were generated using Nanotube Modeller software (http://www.jcrystal.com/products/wincnt/index.htm). Generated SWCNTs were further oxidized using the Builder tool, provided by Pymol[6] visualization software. AutoDockTools (ATD) package (http://autodock.scripps.edu/resources/adt) was further used for formatting and converting the protein data bank (PDB) files into pdbqt format. The docking studies were performed using the center of the EPO as the grid center and a grid box of size 90 Å × 90 Å × 90 Å. The resulting binding poses were clustered together to estimate the number of total binding poses on EPO in each case. The lowest binding energy conformations in each cluster were considered for further analysis.

6. **Generation of murine bone marrow-derived eosinophils.** Bone marrow derived eosinophils were generated as described previously.[7] Briefly bone marrow cells were collected from the femurs and tibiae from BALB/c mice. The erythrocyte depleted bone marrow cells were cultured at 10^6/ml in RPMI 1640 (Invitrogen, Paisley, UK) with 10% FBS (Cambrex, East Rutherford, USA), 2 mM glutamine (Invitrogen, Carlsbad, CA), 25 mM HEPES (Invitrogen), and 1 mM sodium pyruvate (Invitrogen), and 50 µM 2-mercaptoethanol (Sigma-Aldrich, St. Louis,

MO) supplemented with 100 ng/ml recombinant mouse stem cell factor (SCF; Immunotools, Friesoythe, Germany) and 100 ng/ml recombinant mouse FLT3 ligand (FLT3-L; Immunotools). On day four, the medium containing SCF and FLT3-L was replaced with medium containing 10 ng/ml recombinant mouse IL-5 (Immunotools). Four days later, the cells were moved to new flasks and maintained in fresh medium supplemented with rmIL-5. The medium was replaced every second day with fresh medium containing rmIL-5. Mature eosinophils express the integrin chain CD11 and the cell surface antigen, Siglec-F, orthologous of human Siglec-8, predominantly expressed by mouse eosinophils. These proteins were detected with Siglec F PE (BD Biosciences, San Diego, CA) and CD11b FITC (Biolegend, San Diego, CA) by FACSort (BD Biosciences, San Diego, CA). Cells displaying Siglec F+CD11b+ greater than 85% were used for biodegradation experiments. All mice were housed under standard conditions at the Department of Microbiology, Tumor and Cell Biology, Karolinska Institutet, Stockholm. All animal procedures were performed under Stockholm North Ethical Committee for Animal Welfare guidelines (ethical committee approval: Dnr 339/09).

7. **Measurement of eosinophil peroxidase activity.** Detection of eosinophil peroxidase (EPO) released in response to challenge with PAF or lysoPAF (Sigma-Aldrich) was essentially as described.[8] Stock solutions of PAF (P4904, β-Acetyl-γ-O-hexadecyl-L-α-phosphatidylcholine) and lysoPAF (L5016, 1-O-Palmityl-sn-glycero-3-phosphocholine) were prepared at 1 or 10 mM in DMSO and used as indicated; cytochalasine B at 10 mg/ml in DMSO. All subsequent dilutions were prepared in RPMI 1640. Cells were collected by centrifugation and resuspended in RPMI 1640, without phenol red, at 250000 cells/ml; 100 µl was used per well,

unless otherwise indicated. One microliter of secretagogue or vehicle control was added to achieve the indicated concentrations, and cells were incubated at 37°C, 5% CO_2 for 1 h. The cells were eliminated by centrifugation. EPO activity was measured using 100 µl of supernatant, and mixing with 100 µl O-phenylenediamine reagent (800 ml 5 mM O-phenylenediamine in 4 ml 1M Tris [pH 8], 5.2 ml H_2O, and 1.25 ml 30% H_2O_2). The reaction was terminated by the addition of 50 µl 3 M H_2SO_4 to each well and read at 492 nm. In addition to the wells containing the secretagogue to be evaluated, each plate contained a set of cells that remained untreated and a set of wells in which the cells were lysed in 0.2% $NaDodSO_4$ (SDS; KD Medical, Columbia, MD) to determine the total EPO activity. Data are reported as the percentage of total EPO [(absorbance of stimulated sample – no treatment) x 100/total EPO from SDS-lysed cells]. All data are presented as mean ± SD.

8. **Incubation of carbon nanotubes and eosinophils.** Twenty µg of nanotubes were exposed to 20 million activated eosinophils (1 million cells /ml) in culture flasks (50ml). Lyso-PAF 6 µM and Cytochalasine B 5 µg/ml has been added every 6 h to stimulate the eosinophil degranulation. After incubation during 48 h at 37^{o}C the suspensions were centrifugated (3400 rpm, 1h) and resuspended in sterile Ca^{2+}+Mg^{2+}-free phosphate-buffered saline (PBS) vehicle. Samples were further subjected to sonication for 1 h using the ultrasonic probe tip sonicator (Soniprep 150, 20 kHz), and washed in PBS (3400 rpm, 1 h) in order to remove cellular components prior to assessment of carbon nanotube degradation.

9. **Assessment of carbon nanotube biodegradation by eosinophils. Transmission electron microscopy.** 3 µl of aliquots from samples were directly placed on grids

for 5 min. Excess liquid was removed by touching the grid to a filter paper and then allowed to dry. Grids were examined in a Tecnai 12 Spirit Bio TWIN transmission electron microscope (Fei Company, Eindhoven, The Netherlands) at 100 kV. Digital images were taken by using a Veleta camera (Olympus Soft Imaging Solutions, GmbH, Münster, Germany). **Infrared spectroscopy.** The vis-NIR spectra was obtained from the samples using a PerkinElmer Lambda 750 UV/Vis/NIR spectrophotometer. **Raman spectrometry and confocal Raman microscopy.** The measurements were performed with a WITec alpha300 system in combination with a 532 nm laser for excitation and a 100x objective with an NA of 0.95. This results in a lateral resolution of 500 µm and a vertical resolution of 600 µm. The integration time per Raman spectrum varied between 60 and 200 ms. Confocal Raman microscopy combines two different techniques, namely confocal microscopy and Raman spectrometry. Performing Raman microscopy, a Raman spectrum is recorded on every image pixel. Raman spectra between 1327 and 1819 cm^{-1} were collected with a 2.33 cm^{-1} resolution. Raman intensity maps indicating the intensity of the D-band at 1340 cm^{-1} and G-band at 1580 cm^{-1} were obtained to highlight the presence of degraded and non-degraded carbon nanotubes, respectively. Only one single peak was used to calculate the image. For the software utilized (WITec control) it is standard to draw a baseline for this single peak (4 pixels left and right of the chosen area) before integrating, and the resulting baseline is then subtracted. After Raman intensity measurement of all pixels from each sample the corresponding average spectra were calculated.

10. Statistics. The results are presented as mean ± S.D. values from three experiments, and statistical analyses were performed using Student's t-test. The statistical significance of differences was set at $p < 0.05$.

References

[1] J. D. Thompson, D. G. Higgins, T. J. Gibson, *Nucleic Acids Res.* **1994**, *22*, 4673–4680.

[2] A. Sali, L. Potterton, F. Yuan, H. van Vlijmen, M. Karplus, *Proteins* **1995**, *23*, 318–326.

[3] M. A. Martí-Renom, A. C. Stuart, A. Fiser, R. Sánchez, F. Melo, A. Sali, *Annu Rev Biophys Biomol Struct* **2000**, *29*, 291–325.

[4] O. Trott, A. J. Olson, *J Comput Chem* **2010**, *31*, 455–461.

[5] V. E. Kagan, N. V. Konduru, W. Feng, B. L. Allen, J. Conroy, Y. Volkov, I. I. Vlasova, N. A. Belikova, N. Yanamala, A. Kapralov, Y. Y. Tyurina, J. Shi, E. R. Kisin, A. R. Murray, J. Franks, D. Stolz, P. Gou, J. Klein-Seetharaman, B. Fadeel, A. Star, A. A. Shvedova, *Nat Nanotechnol* **2010**, *5*, 354–359.

[6] Pymol software [http://www.pymol.org]

[7] K. D. Dyer, J. M. Moser, M. Czapiga, S. J. Siegel, C. M. Percopo, H. F. Rosenberg, *J. Immunol.* **2008**, *181*, 4004–4009.

[8] D. J. Adamko, Y. Wu, G. J. Gleich, P. Lacy, R. Moqbel, *J. Immunol. Methods* **2004**, *291*, 101–108.

Supplementary Figures

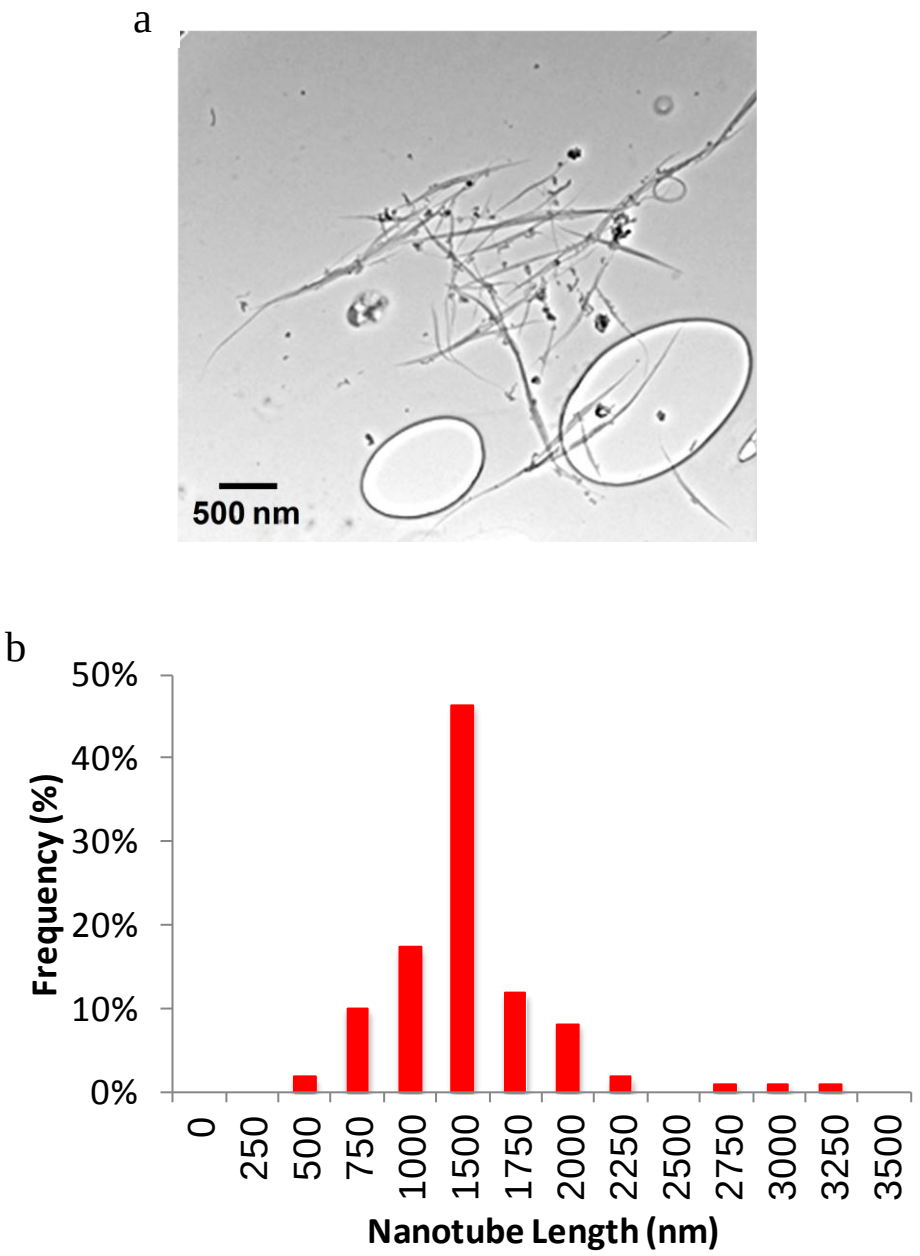

Figure S1. Characterization of SWCNTs employed in the study. (a) Micrograph and (b) histogram of length distribution for single-walled carbon nanotubes (SWCNTs) that underwent oxidation in 3:1 H_2SO_4:HNO_3 for 40 minute obtained by transmission electron microscopy (TEM). The average SWCNT length was 1254 ± 479 nm with a sample size of 110 SWCNTs.

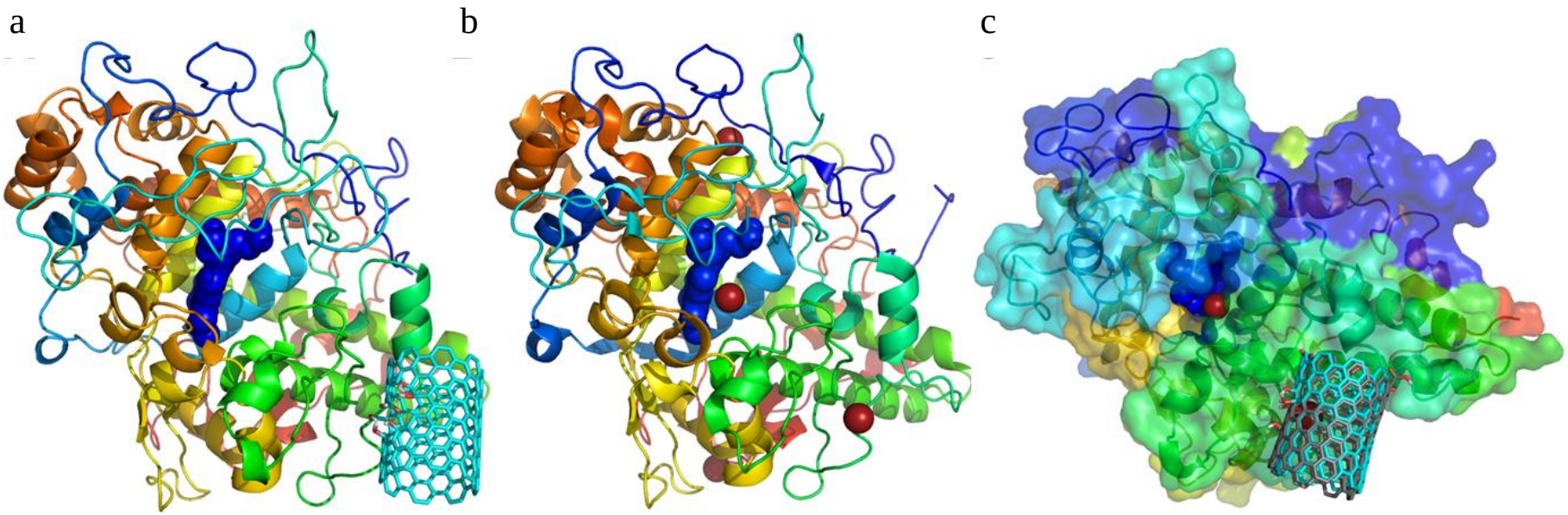

Figure S2. Structural comparison of the predicted interaction sites of oxidized SWCNTs on EPO. (a) Predicted binding site 1 for the oxidized SWCNTs modified in the middle. (b) Crystal structure of myeloperoxidase showing the four Br- ion binding sites. Bromide ions are rendered as spheres and colored in red. (c) An overlay of oxidized SWCNTs modified at the edges and in the middle along with the bromide ion binding sites. The structures of EPO and MPO in (a) and (b), respectively, are colored in rainbow from N-C terminus and represented in cartoon. In (c) the structure of EPO is represented as surface to show the proximity of binding site 1 to the opening of the catalytic site of the peroxidase enzyme.

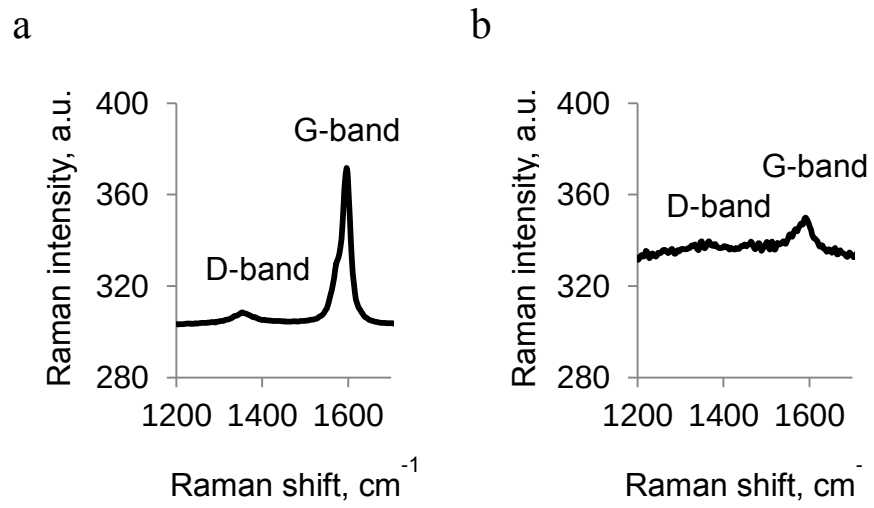

Figure S3. Average spectra obtained from the Raman spectral images. (a,b) Average spectra of ethanol-dried SWCNTs with their corresponding G- and D-bands from (a) non-eosinophil treated and (b) eosinophil treated nanotubes. CNTs incubated with activated eosinophils show loss of the characteristic G-band, followed by appearance of the D-band over time. Cells were activated as described in the legend to Figure 4 and the samples were evaluated after 48 h of incubation with or without cells.

Supplementary Table

Table S1. The possible interaction sites of SWCNTs on EPO. A list of all residues that stabilize the two binding sites along with the lowest binding energy and the total number of conformations (out of 9 top conformations listed as "#") observed in each case is listed. The positively charged residues that stabilize the oxidized groups of SWCNTs are highlighted in bold.

	SWCNTs oxidized at the edge			SWCNTs oxidized in the middle		
	Predicted Binding Energy (Kcal/mol)	#	Residues	Predicted Binding Energy (Kcal/mol)	#	Residues
Site 1	-15	3	**Arg205**, Leu206, **Arg207**, Asn208, **Arg209**, Thr210, Ala217, Gln220, Arg221, Pro231, Phe232, Asn234, Leu253	-12.6	2	Arg205, Arg207, Asn208, Arg209, Thr210, Ala217, Asn219, Gln220, **Arg221**, Pro231, Phe232, Asp233, Asn234, Leu253
Site 2	-14.7	4	**Arg94**, Leu95, Thr96, Ser97, **Arg99**, Gln359, Phe363, Leu365, Tyr369, Arg370, Ala371, His377, Thr406, Pro407	-12.5	6	Leu95, Thr96, Ser97, **Arg99**, Gln359, Phe363, Leu365, Tyr369, Arg370, Ala371, His377, Ser376, Ala405, Thr406, Pro407,